

Synthesis of Doubly Strapped *meso-meso*-Linked Porphyrin Arrays and Triply Linked Conjugated Porphyrin Tapes

Toshiaki Ikeda,^[a] Juha M. Lintuluoto,^[a] Naoki Aratani,^[a] Zin Seok Yoon,^[b]
Dongho Kim,^{*[b]} and Atsuhiko Osuka^{*[a]}

Keywords: Conjugation / Encapsulation / Molecular wires / Oligomerization / Porphyrinoids

1,10-Dioxydecamethylene doubly strapped Zn^{II}-porphyrin **S1** was prepared and treated with AgPF₆ to give *meso-meso*-linked porphyrin oligomers **Sn** ($n = 2, 3, 4, 6, 8$, and 12), which were converted to triply linked porphyrin tapes **TSn** by *meso,meso'*-dibromo *meso-meso*-linked porphyrin arrays **BSn** and *meso,meso'*-diphenyl *meso-meso*-linked porphyrin arrays **PSn**. The structures of **S1** and **S2** have been determined by single-crystal X-ray diffraction analysis. Characteristically, **Sn** exhibit sharp Q(0,0) absorption and fluorescence

bands. Low energy Q-band-like absorption bands of **TSn** are progressively red-shifted with an increase in the number of porphyrins without saturation behavior of conjugation. The double straps suppress π - π stacking to some extent as seen from partial preservation of vibration structures in the Q-band-like bands of **TS4** and **TS6** and improve the chemical stabilities of longer tapes such as **TS8** and **TS12**.

(© Wiley-VCH Verlag GmbH & Co. KGaA, 69451 Weinheim, Germany, 2006)

Introduction

Organic molecules with extended π -conjugated systems have attracted considerable interest because of their possible applications to organic conducting materials, non-linear optical (NLO) materials, near-infrared (near-IR) dyes, and molecular wires.^[1,2] Extensive synthetic efforts have been made towards such conjugated molecular systems, but have often encountered serious problems such as synthetic difficulty, chemical instability, and poor solubility with increasing size of π -conjugated systems. Besides these, there is an intrinsic problem of saturation as characterized by effective conjugated length "ECL". ECL defines the extent of π -conjugated systems in which the electronic delocalization is limited, and at which point the optical, electrochemical, and other physical properties reach a saturation level that is common with the analogous polymer.^[1a,3] Therefore, it is important to circumvent the ECL problem, particularly for exploration of highly conjugated molecules that may serve as molecular wires.

Porphyrin, a tetrapyrrolic pigment with 18π -electron conjugated system, has been used in a variety of fields including reaction catalysts, artificial photosynthesis, photodynamic therapy, sensors, and so on.^[4] Electronic properties of porphyrins are susceptible to chemical modifications at the periphery. This characteristic has been used, through the attachments of unsaturated segments to a porphyrinic π network, to create conjugated porphyrins that exhibit rather altered optical and electrochemical properties.^[5–10] Recently, we have explored *meso-meso*, β - β , β - β triply linked porphyrin arrays (porphyrin tapes),^[11] which are unprecedented in respect of the extend of π conjugation, in that their absorption spectra exhibit the progressive red-shifts, reaching an exceptionally red-shifted absorption band at 2800 nm for the dodecameric porphyrin tape.^[11d] This feature is intriguing, since they do not exhibit a saturation behavior up to the dodecamer, indicating that ECL of these arrays is at least larger than 12. Thus, this direct triple linkage may serve as an effective platform to overcome the ECL problem. In addition, the triply linked porphyrin tapes have been used for functional conjugates with C₆₀^[12] and interesting supramolecular interactions by taking advantages of their unique electronic properties.^[13] Despite these promises, the porphyrin tapes have problems of poor solubility, strong stacking tendency, and chemical instability, which become more serious with increasing number of porphyrin subunits.

In this paper, we report the synthesis of doubly strapped porphyrin tapes, which has been designed to increase chemical stability and improve solubility in common organic solvents. In recent years, similar encapsulating strategy has been demonstrated to be effective for the isolation of molec-

[a] Department of Chemistry, Graduate School of Science, Kyoto University, and Core Research for Evolutional Science and Technology (CREST), Japan Science and Technology Agency (JST), Sakyo-ku, Kyoto 606-8502, Japan
Fax: +81-75-753-3970
E-mail: osuka@kuchem.kyoto-u.ac.jp

[b] Center for Ultrafast Optical Characteristics Control and Department of Chemistry, Yonsei University, Seoul 120-749, Korea
Fax: +82-2-2123-2434
E-mail: dongho@yonsei.ac.kr

Supporting information for this article is available on the WWW under <http://www.eurjoc.org> or from the author.

ular wires, which then acquire improved solubilities as well as enhanced emission quantum yields.^[14]

Results and Discussions

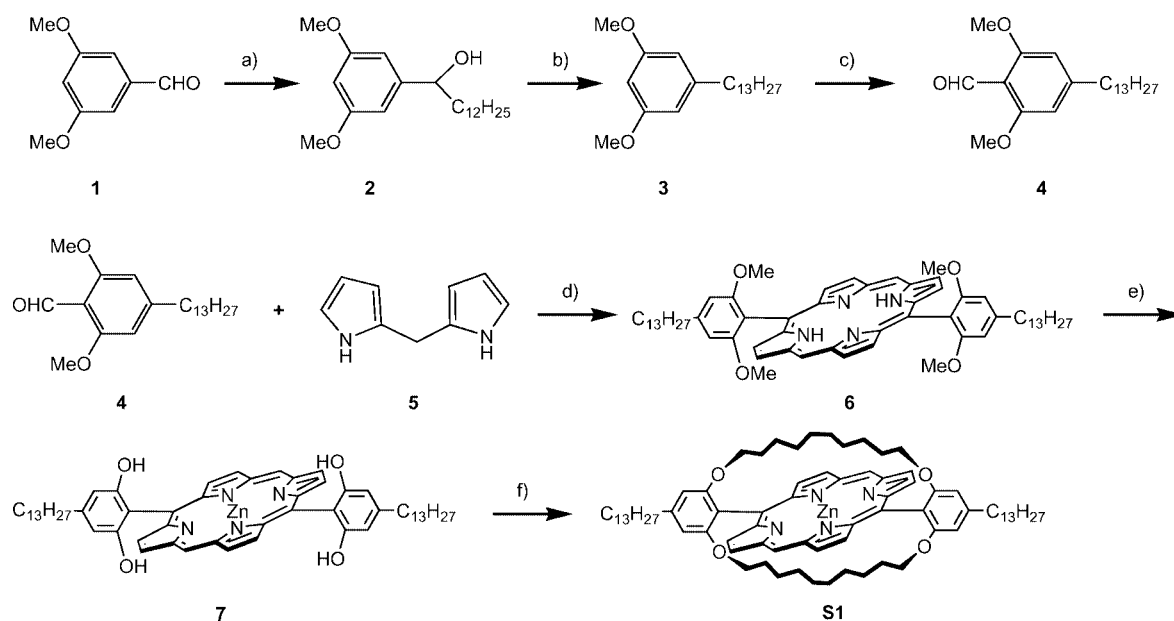
The doubly strapped porphyrin **S1** was synthesized as shown in Scheme 1. 2,6-Dimethoxy-4-tridecylbenzaldehyde (**4**) was prepared from commercially available 3,5-dimethoxybenzaldehyde (**1**) in 35% yield in three steps. Acid-catalyzed condensation of the aldehyde **4** and the dipyrromethane (**5**) followed by DDQ oxidation provided 5,15-bis(2,6-dimethoxy-4-tridecylphenyl)porphyrin (**6**) in 30% yield. Demethylation of **6** with BBr_3 followed by Zn^{II} -ion insertion gave the porphyrin **7** in 98% yield in two steps. Double-strapping reaction of **7** with 1,10-dibromodecane was carried out in acetone in the presence of K_2CO_3 under reflux for 20 days^[15] to give **S1** in 62% yield. Doubly strapped porphyrin **S1** exhibited the parent molecular ion peak at $m/z = 1229.77$ (calcd. for $\text{C}_{78}\text{H}_{109}\text{N}_4\text{O}_4\text{Zn}$, 1229.77) in the ESI-TOF mass spectrum. The 600-MHz ^1H NMR spectrum of **S1** in CDCl_3 exhibited a singlet for H_{meso} at $\delta = 10.22$ ppm, a set of mutually coupled doublets for the peripheral β -protons H_β^1 and H_β^2 at $\delta = 9.37$ and 9.11 ppm, and a singlet for H_{aryl} at $\delta = 6.98$ ppm (proton designations are shown in Figure 1). Characteristically, the protons of the strap alkyl chain were observed in a shielded region; H^a at $\delta = 3.75$ ppm, H^b at $\delta = 0.65$ ppm, H^c at $\delta = -1.34$ ppm, H^d at $\delta = -1.44$ ppm and H^e at $\delta = -2.48$ ppm due to the aromatic ring current of the porphyrin, hence indicating the location of the straps just above the porphyrin ring.

The molecular structure of **S1** was confirmed by X-ray crystallography. X-ray-quality crystals of **S1** were obtained by slow diffusion of acetonitrile into a CHCl_3 solution of **S1**. The structure of **S1** shows an almost symmetric conformation with respect to the porphyrin plane, where the por-

phyrin ring is covered by the two 1,10-dioxydecamethylene straps that take an *anti*-staggered conformation with an average separation of 4.1 Å from the porphyrin plane (Figure 2). In the crystal, the distance between the nearest two porphyrins is about 7.91 Å without any significant intermolecular π - π interaction.

Ag^{I} -promoted *meso-meso* coupling reaction is usually conducted by treatment of a 5,15-diaryl- Zn^{II} -porphyrin with a slightly excess amount of AgPF_6 in CHCl_3 at room temperature for several hours (Scheme 2).^[16] We first tried the coupling reaction of **S1** under the standard conditions (1.5 equiv. of AgPF_6 and at 30 °C), which however did not provide any coupling product. In contrast, under the same conditions, the coupling reaction of **M1** that is a strap-free analogue of **S1** proceeded extensively to provide highly oligomerized products within 1 h. At lower temperature (0 °C), the coupling reaction of **M1** gave *meso-meso*-linked porphyrin dimer **M2** (14%), trimer **M3** (22%), tetramer **M4** (10%), pentamer **M5** (6%), hexamer **M6** (4%), and heptamer **M7** (trace) along with recovery of **M1** (28%) in a cleaner manner. Since this coupling reaction is believed to be initiated by the one-electron oxidation of a porphyrin by Ag^{I} ion,^[16] the first one-electron oxidation potential of the porphyrin should be an important parameter. Cyclic voltammetry has revealed that the oxidation potential of **S1** is 0.29 V vs. ferrocene/ferrocenium ion, which is lower than that (0.32 V) of **M1**. Thus, the observed low reactivity of **S1** is considered to be not an electronic but a steric reason. Probably, steric hindrance imposed by the double straps suppresses the approach of Ag^{I} ion to the porphyrin plane in **S1**.

We thus examined the coupling reaction of **S1** under stronger conditions by changing the amount of AgPF_6 , reaction temperature, and reaction time. In the meanwhile, we found that the coupling reaction of **S1** in CHCl_3 proceeded



Scheme 1. Synthesis of **S1**. a) $\text{C}_{12}\text{H}_{25}\text{MgBr}$, Et_2O , 92%. b) NaBH_3CN , TFA, CH_2Cl_2 , 71%. c) 1) BuLi , Et_2O , 2) DMF, 62%. d) 1) TFA, CH_2Cl_2 , 2) DDQ, 30%. e) 1) BBr_3 , CH_2Cl_2 , 2) $\text{Zn}(\text{OAc})_2 \cdot 2\text{H}_2\text{O}$, MeOH, 98%. f) $\text{Br}-(\text{CH}_2)_{10}-\text{Br}$, K_2CO_3 , acetone, 62%.

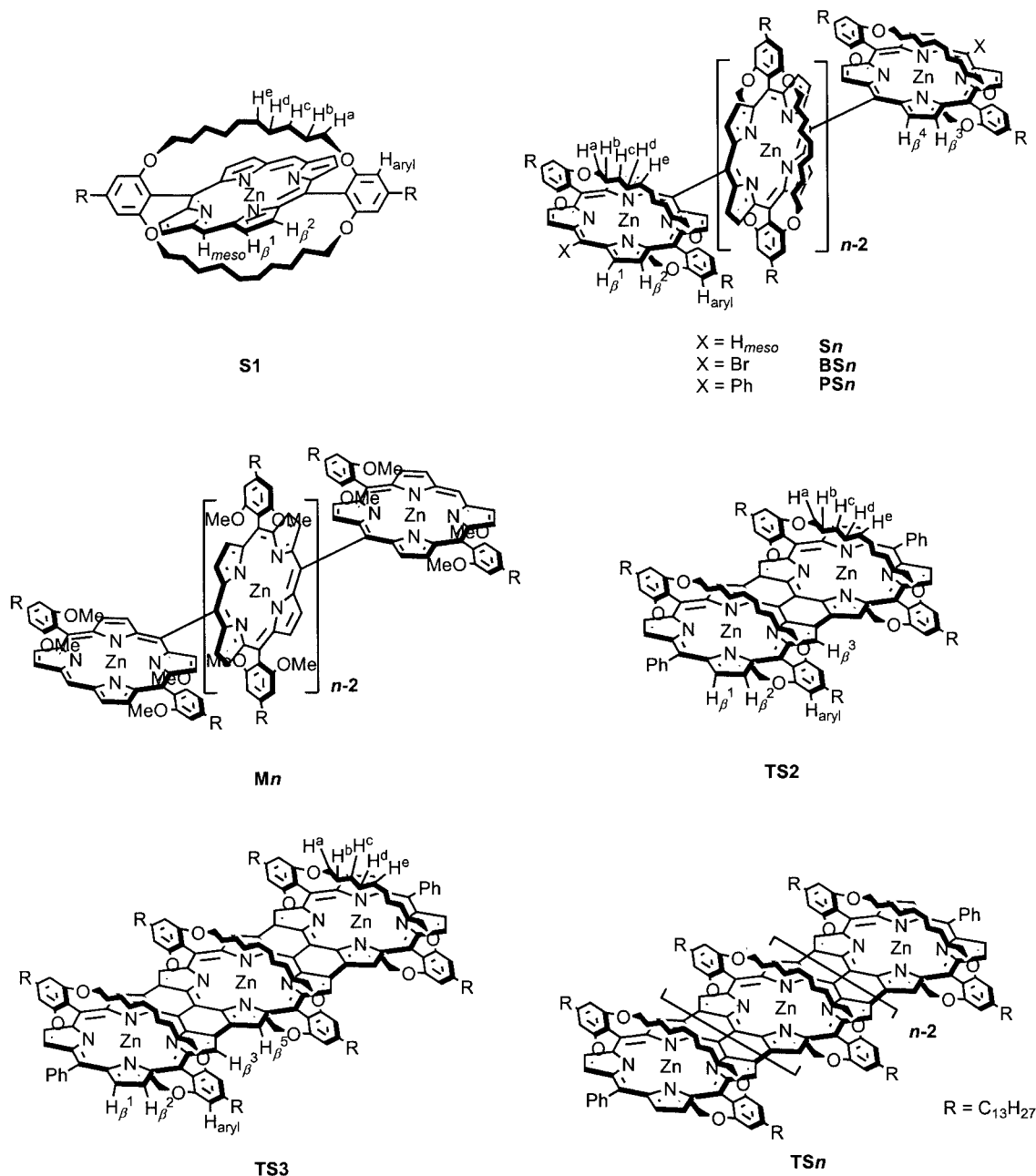


Figure 1. Structures of porphyrins studied in this paper and proton designations.

at reflux in the presence of 4 equiv. of AgPF₆ for 2 days. Under these conditions, the coupling reaction of **S1** provided doubly strapped *meso-meso*-linked porphyrin dimer **S2** (21%), trimer **S3** (3%), and tetramer **S4** (trace) along with recovery of **S1** (52%). The similar reaction of **S2** afforded **S4** (21%), **S6** (4%), and **S8** (trace) along with recovery of **S2** (57%). However, the similar reaction for **S4** gave only a small amount of **S8** (2%) along with recovery of **S4** (32%). The poor material balance suggested that **S4** and its coupling arrays might be unstable under these reaction conditions. Lowering the reaction temperature to 45 °C led to better yields; **S8** (10%), **S12** (5%), and **S16** (trace) along with recovery (33%) of **S4**. The coupling of the doubly strapped Zn^{II} porphyrin substrates **Sn** needs elevated tem-

perature in the presence of Ag^I salt, under which conditions the longer **Sn** may be not tolerant. This situation makes elongation of **Sn** to long porphyrin arrays quite a difficult task, which is different from the previously reported non-strapped series.^[16]

The *meso-meso*-linked oligomers **Sn** thus prepared have been characterized by ¹H NMR, MALDI-TOF mass, UV/Vis absorption, and fluorescence spectroscopy. MALDI-TOF mass spectrometry was very effective for the detection of the parent molecular ion peaks of **Sn** at the expected positions. The ¹H NMR spectrum of **S2** in CDCl₃ provided a singlet at δ = 10.25 ppm for H_{meso}, two sets of mutually coupled doublets for H _{β 1} and H _{β 2} at δ = 9.40 and 9.10 ppm, and for H _{β 3} and H _{β 4} at δ = 8.64 and 8.05 ppm, a singlet at

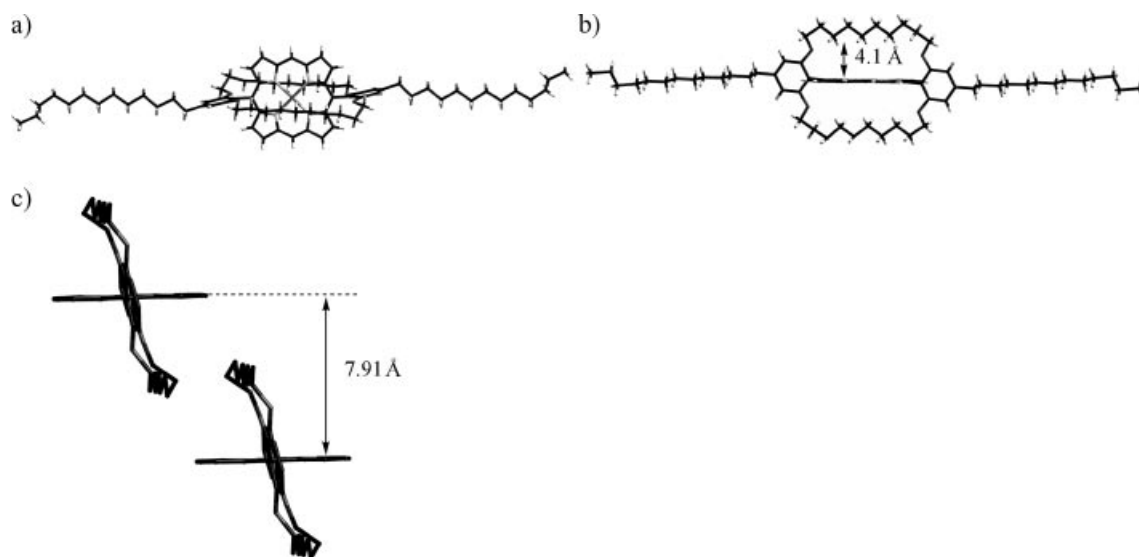
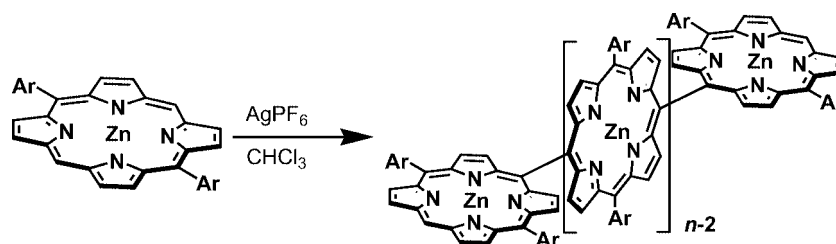


Figure 2. X-ray crystal structure of **S1**. a) Top view, b) side view, and c) crystal packing pattern. Some atoms were omitted for clarity.



Scheme 2. Ag^{I} -promoted *meso-meso* coupling reaction of a 5,15-diaryl-substituted Zn^{II} porphyrins.

$\delta = 6.89$ ppm for H_{aryl} , a series of multiplets at $\delta = 3.75$ ppm for H^{a} protons, at $\delta = 0.77$ ppm for H^{b} proton, at $\delta = -1.01$ ppm for H^{c} proton, at $\delta = -1.25$ ppm for H^{d} proton, and at -2.17 ppm for H^{e} protons. The protons of the straps were observed essentially at the same chemical shifts as those of **S1** except for slight down-field shifts for H^{a} , H^{b} , and H^{c} due to the ring current of neighboring porphyrin, implying that the aromatic ring current of the porphyrin monomer **S1** is well preserved in **S2**. Similar trends were observed for higher oligomers **Sn**.

X-ray-grade crystals of **S2** were grown by vapor diffusion of acetonitrile into its CH_2Cl_2 solution. The solid-state structure determined with these crystals shows that the two straps, similar to the case of **S1**, are lying over and below the porphyrin macrocycle with an average 4.0 \AA separation from the porphyrin ring and a dihedral angle between two porphyrin planes of 70.3° (Figure 3, a, b). This small dihedral angle between the diporphyrins may be caused by the strong and tight crystal packing in the crystal. In the crystal, **S2** molecules are packed with its porphyrin planes being parallel with those of neighboring **S2** molecules with interplanar distances of ca. 6.6 \AA and 7.3 \AA (Figure 3, c).

The *meso-meso*-linked porphyrin arrays **Sn** were converted to triply linked porphyrin tapes **TSn** by the synthetic protocol involving *meso*-bromination, *meso*-phenyl capping reaction, and oxidative ringclosure (Scheme 3).^[11d] Treatment of **Sn** with NBS resulted in nearly quantitative re-

giosselective *meso,meso'*-dibromination to afford **BSn** (82–96%), which in turn were converted to *meso,meso'*-diphenyl-capped arrays **PSn** through Suzuki–Miyaura cross coupling with phenyl boronic acid (78–94%). The ^1H NMR spectrum of **S4** exhibits a singlet at $\delta = 10.29$ ppm due to H_{meso} and mutually coupled doublets at $\delta = 9.44$ and 9.15 ppm due to H_{β}^1 and H_{β}^2 protons, while that of **BS4** lacks singlet signal due to H_{meso} and shows doublets at $\delta = 9.81$ and 9.05 ppm due to H_{β}^1 and H_{β}^2 that are down-field shifted due to the bromine atoms attached at the *meso* positions. In the ^1H NMR spectrum of **PS4**, signals due to H_{β}^1 and H_{β}^2 protons appear at $\delta = 8.97$ and 8.96 ppm, reflecting a local deshielding effect of the phenyl group at the *meso* positions. The protons of the strapped chains in **BSn** and **PSn** appear at nearly the same positions as those in **Sn**.

The oxidation of **PSn** with DDQ- $\text{Sc}(\text{OTf})_3$ in toluene at 80°C for 2 h provided doubly strapped triply linked porphyrin tapes **TSn** in good yields (62–94%). MALDI-TOF mass spectroscopy revealed the parent ion peaks for **TS2** at $m/z = 2598.64$ (calcd for $\text{C}_{168}\text{H}_{218}\text{N}_8\text{O}_8\text{Zn}_2$; $m/z = 2608.29$), **TS3** at $m/z = 3825.16$ (calcd for $\text{C}_{246}\text{H}_{320}\text{N}_{12}\text{O}_{12}\text{Zn}_3$; $m/z = 3833.30$), and **TS4** at $m/z = 5048.66$ (calcd for $\text{C}_{324}\text{H}_{422}\text{N}_{16}\text{O}_{16}\text{Zn}_4$; $m/z = 5058.32$), but the parent ion peaks of higher porphyrin tapes could not be detected by this method. The ^1H NMR spectrum of **TS2** in CDCl_3 exhibited a set of mutually coupled doublets for H_{β}^1 and H_{β}^2 at $\delta = 7.62$ ppm and 7.60 ppm, a singlet for H_{β}^3 at $\delta =$

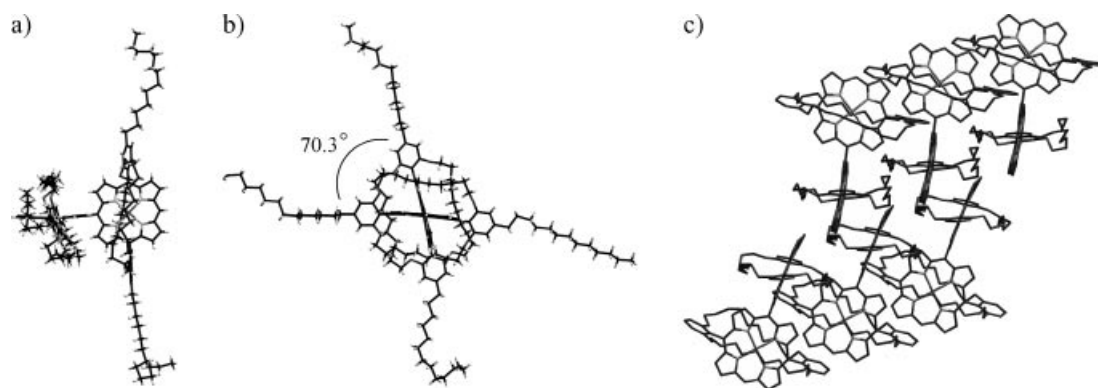
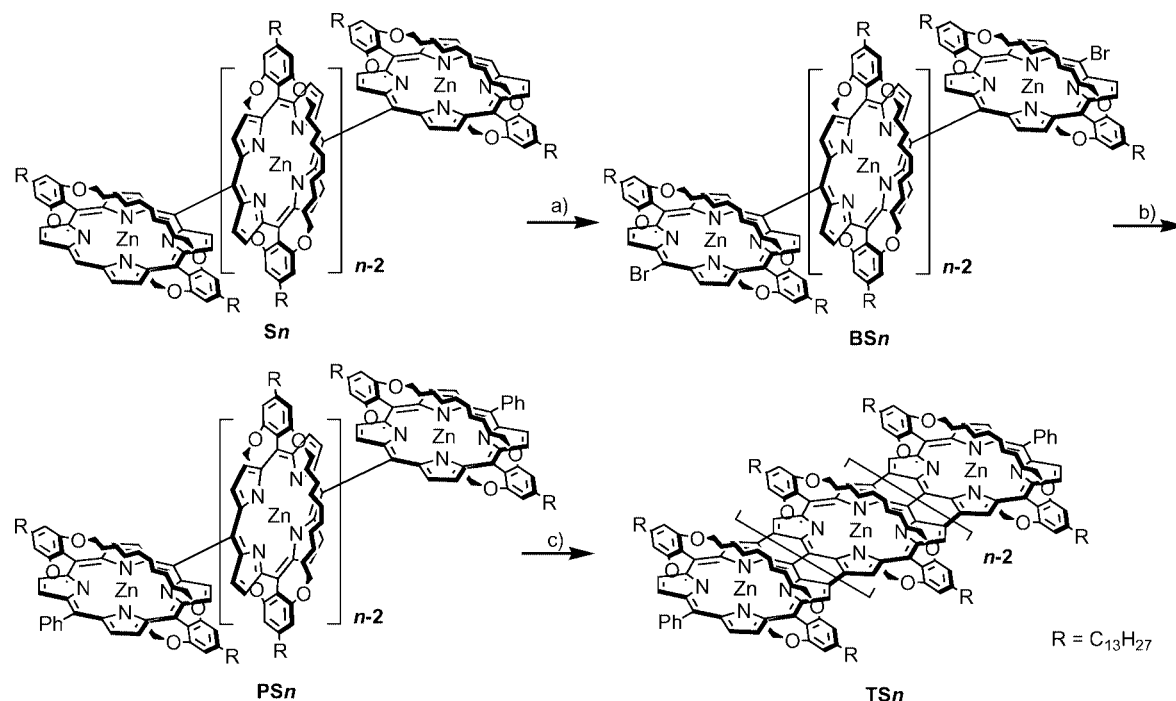


Figure 3. X-ray crystal structure of **S2**. a) Top view, b) side view, c) crystal packing pattern. Some atoms were omitted for clarity.



Scheme 3. Synthesis of triply linked porphyrins **TSn**. a) NBS, pyridine, CHCl_3 , 83–96% b) PhB(OH)_2 , $\text{Pd(PPh}_3)_4$, K_2CO_3 , toluene, 79–94%. c) DDQ, Sc(OTf)_3 , toluene, 62–95%.

7.24 ppm, and a set of signals due to the strap protons; H^a at $\delta = 3.88$ and 3.82 ppm, H^b at $\delta = 1.14$ ppm, H^c at $\delta = 0.13$ ppm, H^d at $\delta = 0.05$ ppm and H^e at $\delta = -0.38$ ppm. These chemical shifts indicated an attenuated diatropic ring current of porphyrin rings in **TS2** as compared with that in **S2**, as the peripheral protons were shifted to high field and the strap protons were shifted to low field. The ^1H NMR spectrum of **TS3** was very broad at room temperature but became sharper at 60 °C, showing broad peaks at $\delta = 7.47$ ppm for H_β^1 and H_β^2 , $\delta = 7.04$ ppm for H_β^3 , $\delta = 6.34$ ppm for H_β^5 , $\delta = 3.89$, 3.75, and 3.67 ppm for H^a , $\delta = 0.76$ ppm for H^b , -0.14 ppm for H^c and H^d , and $\delta = -0.74$ ppm for H^e . Unfortunately, ^1H NMR spectra of higher porphyrin tapes ($> \text{TS4}$) were quite broad and almost useless for the structural characterizations. This has been interpreted in terms of incomplete encapsulation of

the porphyrin π planes of higher porphyrin tapes by the present double alkyl strap.^[11e,11f]

The absorption spectra of **Sn** in CHCl_3 are shown in Figure 4. Similar to the previously reported *meso-meso*-linked porphyrin oligomers,^[16] **Sn** exhibit split Soret bands and red-shifted Q bands. Of the split two Soret bands, the high-energy band remains in the same position as that of **S1**, and the other low-energy band is progressively red-shifted as the number of porphyrins increases. These split Soret bands can be understood in terms of the exciton coupling theory in essentially the same manner as performed for the non-strapped *meso-meso*-linked porphyrin oligomers.^[16–18] As a notable difference from the spectral characteristics of the non-strapped arrays and **Mn**, the lowest energy Q(0,0) bands of **Sn** are observed as sharp bands, which are progressively red-shifted as the number of the porphyrins in-

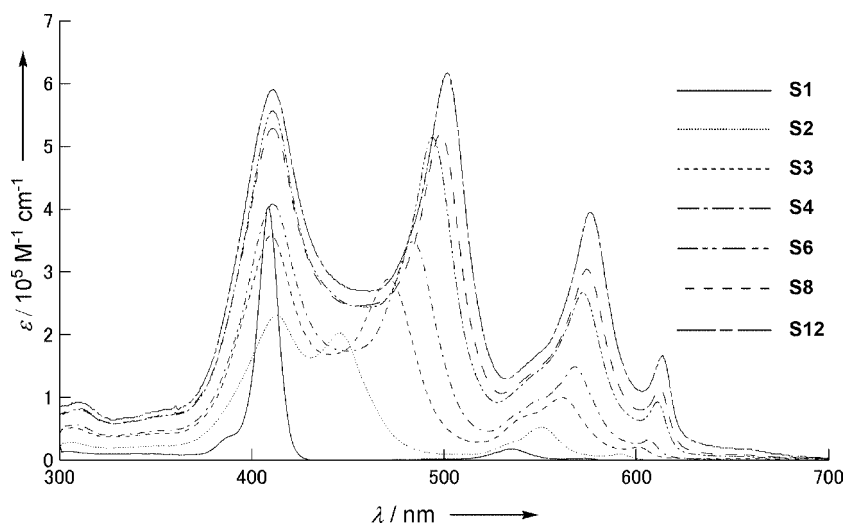


Figure 4. Absorption spectra of **S1**, **S2**, **S3**, **S4**, **S6**, **S8**, and **S12** in CHCl_3 .

creases. The Q(0,0) bands of the non-strapped arrays^[16a] and **Mn** are broad and almost hidden by Q(0,1) vibronic bands (Supporting Information, see also the footnote on the first page of this article).

The fluorescence spectra of **Sn** and **Mn** in CHCl_3 are shown in Figure 5. Whereas the fluorescence spectral shapes of **Mn** are similar to those of the previously reported non-strapped ones in respect of broad band with three bands, **Sn** exhibit remarkably sharp fluorescence spectra with intensified 0–0 bands, particularly for longer arrays > **S4**. The position of the 0–0 band is gradually red-shifted with an increase in the number of porphyrins, and seems saturated at **S8** and **S12**. The red-shifts of the fluorescence Q(0,0) bands correspond to those of the absorption Q-bands. The fluorescence quantum yields of **Sn** determined with respect to $\Phi_F = 0.03$ for Zn tetraphenylporphyrin^[19] are roughly similar to those of **Mn**; **S1**: 0.028, **S2**: 0.038, **S3**: 0.051, **S4**: 0.055, **S6**: 0.066, **S8**: 0.068, **S12**: 0.070, **M1**: 0.031, **M2**: 0.038, **M3**: 0.049, **M4**: 0.063, and **M6**: 0.073. The Φ_F value increases up to **S6** and becomes constant for **S8** and **S12**, which suggests the coherent length of 6–8 porphyrin units for **S1** state of **Sn**, which is similar to that of the non-strapped arrays.^[16a] The enhancement of Q(0,0) absorption bands may be ascribed to the anchoring of *meso*-substituted dialkoxyphenyl groups in **Sn**, because the relatively free motions of *meso*-substituted phenyl groups give rise to stronger vibronic Q(0,1) bands.^[20,21] The restricted rotational freedom caused by the double strap in **Sn** series can modify the vibronic structure in porphyrin monomers compared to **Mn**, which leads to the distinct Q(0,0) absorption and fluorescence bands.

The absorption spectra of **TSn** ($n = 2, 3, 4, 6$, and 8) in CHCl_3 are shown in Figure 6. A clear absorption spectrum of **TS12** was not obtained due to its extremely poor solubility in CHCl_3 or other solvents. Similarly to the previously reported non-strapped porphyrin tapes,^[11] the absorption spectra of **TSn** have main three bands; band I (ca. 400 nm), band II (500–1000 nm), and band III (> 1000 nm). Bands

I are commonly observed around 400 nm at the same position of the Soret band of porphyrin, and bands II are shifted to lower energy with an increase in the number of porphyrins, and bands III are the lowest energy bands and more red-shifted with an increase in the number of porphyrins. The bands I and II have been interpreted as split Soret bands and the bands III have been interpreted as Q-like bands on the basis of several theoretical analyses.^[17,18] Progressive red-shifts of the bands II and III in the present series are similar to those of the non-strapped ones. The bands III of **TS2** and **TS3** show typical vibrational structures of porphyrin consisting of Q(0,0) and Q(0,1) absorption bands, and interestingly those of **TS4** and **TS6** partially preserve such vibrational structures but that of **TS8** is very broad without such structure. In the case of the non-strapped porphyrin tapes, the bands III are broad and structureless for $n \geq 4$.^[11d] These broad bands can be mainly ascribed to π – π interaction on the basis of the previous studies,^[11e,11f] and thus the bands III of **TS4** and **TS6** indicate partial prevention of such π – π interaction by the double strap but the broad band III in **TS8** indicates significant π – π stacking. Figure 7 shows the plots of absorption peak of Q-like band of **TSn** vs. the number of porphyrins n . As noted above, **TSn** show two absorption bands in the band III (**TS2**–**TS6**), but longer tape **TS8** shows a broad band III. Both plots are linear, suggesting that the ECL of **TSn** is at least larger than 8.

Since the electronic absorption bands of **TSn** reach the infrared (IR) region, their IR spectra in KBr pellet were examined (Figure 8). In these spectra, bands due to C–H stretching were observed around 3000 cm^{-1} and broad bands due to O–H stretching of contaminated water were observed around 3600 cm^{-1} . The electronic absorption bands III were actually observed at 6600 cm^{-1} for **TS4**, 5210 cm^{-1} for **TS6**, 4410 cm^{-1} for **TS8**, and 3050 cm^{-1} for **TS12**. Remarkably, the edge of electronic absorption band of **TS12** reaches about 1800 cm^{-1} as a rare example of an electronic absorption band in the IR region. Furthermore,

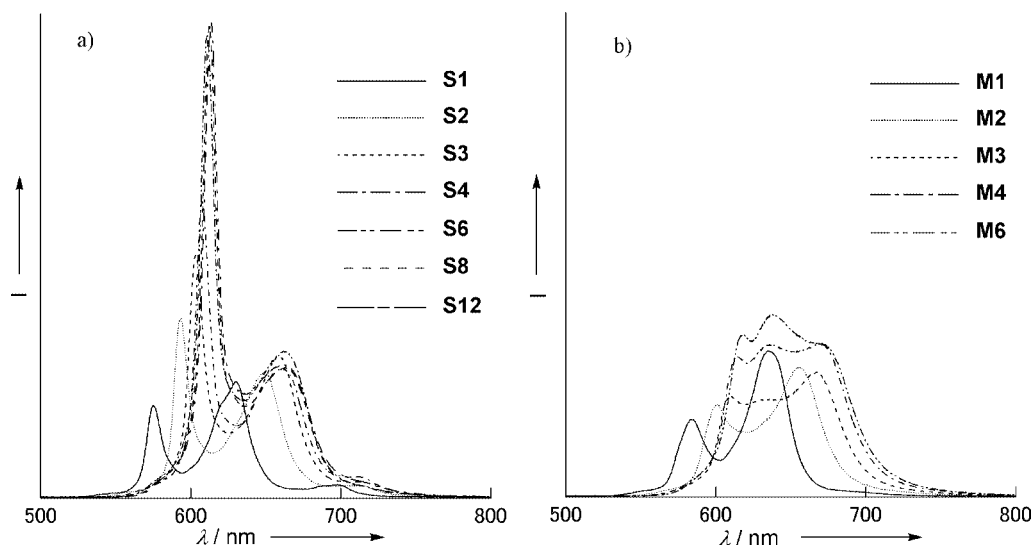


Figure 5. Fluorescence spectra taken for excitation at 411 nm in CHCl_3 . a) S1, S2, S3, S4, S6, S8, and S12. b) M1, M2, M3, M4, and M6.

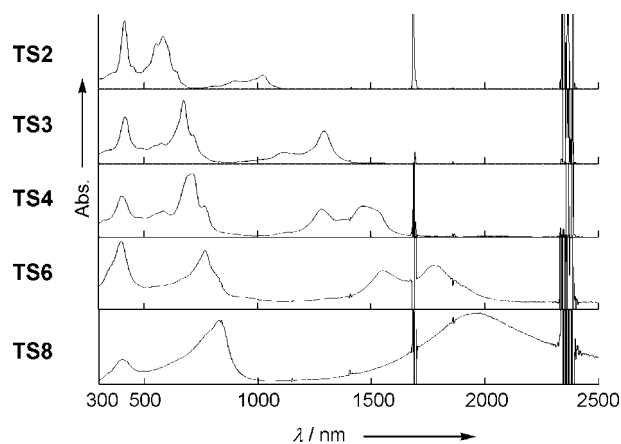


Figure 6. UV/Vis absorption spectra of TS2, TS3, TS4, TS6, and TS8 in CHCl_3 .

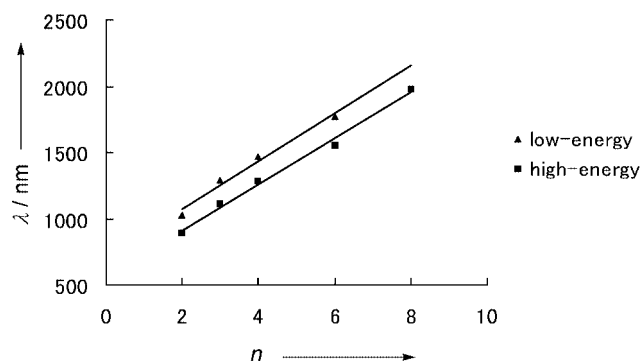


Figure 7. Plots of absorption peak of Q-like band of TS_n in UV/Vis vs. the number of porphyrins n .

it is noteworthy that the shapes of the bands III in the IR spectra of TS_n resemble those of the absorption spectra, and the bands III of TS_8 and TS_{12} possess two bands in contrast to the corresponding electronic absorption band of TS_8 that is only broad. These observations suggest that the

aggregation of TS_n in KBr pellet is not extensive in comparison to that in CHCl_3 . Figure 9 shows the plots of the absorption peak of Q-like band in IR spectra vs. n , which are both linear, indicating the ECL of TS_n larger than 12.

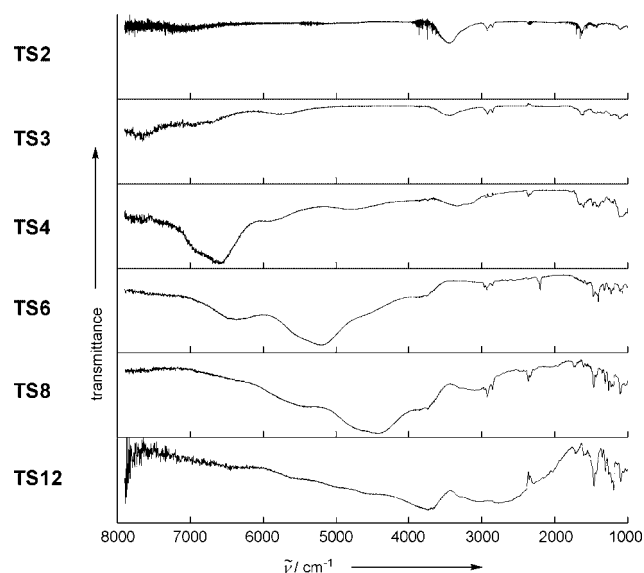


Figure 8. IR spectra of TS2, TS3, TS4, TS6, TS8, and TS12 in KBr pellet.

Finally, it is important to note that the chemical stabilities of TS_n are considerably improved compared with the non-strapped porphyrin tapes. The non-strapped porphyrin tapes octamer and dodecamer were reasonably stable for their separation and manipulations at ambient temperature in the air but faded out slowly during storage in a refrigerator for one or two months. On the other hand, such changes were not observed for TS_8 and TS_{12} under the similar conditions, demonstrating that the double straps improve the chemical stabilities of higher porphyrin tapes.

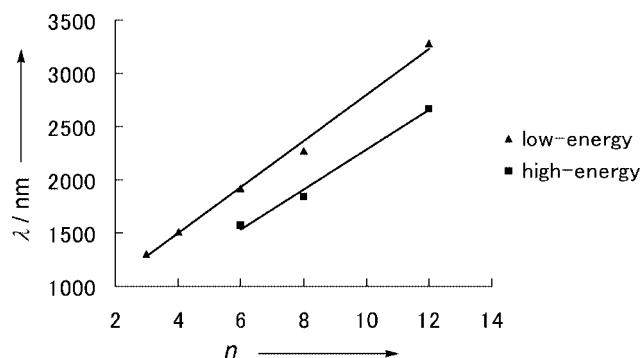


Figure 9. Plots of absorption peak of Q-like band of **TSn** in IR vs. the number of porphyrins *n*.

In summary, the doubly strapped *meso-meso*-linked porphyrin arrays **Sn** and triply linked porphyrin tapes **TSn** were prepared and characterized. The double straps have been shown to cause intensified Q(0,0) bands in the absorption and fluorescence spectra of **Sn** and to suppress the intermolecular π - π interactions and enhance the chemical stabilities of **TSn**.

Experimental Section

General: All reagents and solvents were of commercial reagent grade and were used without further purification except where noted. Dry toluene and dry CH_2Cl_2 were obtained by distillation over CaH_2 . Dry CHCl_3 was obtained by distillation over CaH_2 and purification through a short basic alumina column. ^1H NMR spectra were recorded with a Jeol delta-600 spectrometer, and chemical shifts were reported as the delta scale in ppm relative to CHCl_3 ($\delta = 7.260$ ppm). Spectroscopic-grade CHCl_3 was used as solvent for spectroscopic studies. UV/Visible/NIR absorption spectra were recorded with a Shimadzu UV-3100 spectrometer. Fluorescence spectra were recorded with Shimadzu RF-5300PC spectrometer. IR spectra were recorded with Jasco FT/IR-420 spectrometer. Mass spectra were recorded with a Shimadzu Kratos Kompact Maldi4 using positive-Maldi ionization method with/without 9-nitroanthracene (9NA) matrix, with a Jeol HX-110 spectrometer with the positive-FAB ionization method (accelerating voltage, 10 kV; primary ion sources, Xe) and 3-nitrobenzyl alcohol matrix, and with a Bruker microTOF using positive or negative mode ESI-TOF method of acetonitrile solution. Preparative separations were performed by silica gel flash column chromatography (Merck, Kieselgel 60H, Art. no. 7736), silica gel gravity column chromatography (Wakogel C-400), and size exclusion gel permeation chromatography (Bio-Rad Bio-Beads S-X1, packed with toluene or CHCl_3 in a 4×100 cm gravity flow column; flow rate, $3.8 \text{ mL} \cdot \text{min}^{-1}$). Analytical GPC-HPLC was performed with Jaigel 2.5H-AF, 3H-AF, and 4H-AF columns in series with a Jasco HPLC system using a multi-wavelength detector MD-915. Recycling preparative GPC-HPLC separations were carried out with JAI LC-908 using preparative Jaigel-2.5 H, 3 H, and 4H columns in series. Redox potentials were measured by the cyclic voltammetry method and differential pulse voltammetry method with an ALS electrochemical analyzer model 660. X-ray crystallography was performed on a Rigaku-Raxis imaging plate system (Raxis Rapid).

5-(1-Hydroxytridecyl)-1,3-dimethoxybenzene (2): To a suspension of magnesium turnings (19.8 g, 814 mmol) and a piece of iodine in dry diethyl ether (300 mL) under nitrogen was added dodecyl bromide

(98 mL, 407 mmol) dropwise, and the resulting mixture was stirred until the reaction was finished. A solution of the aldehyde **1** (45.0 g, 271 mmol) in dry diethyl ether (250 mL) was added dropwise to the mixture at 0°C , and the resulting mixture was stirred for 3 h, and then the reaction was quenched by the addition of aqueous ammonium chloride. The organic layer was separated and the aqueous layer was further extracted with diethyl ether. The combined organic layer was washed with brine, dried with anhydrous sodium sulfate, and the solvent was evaporated. Dodecane was removed by vacuum distillation, which induced crystallization of **2** as a colorless solid. Yield 89.9 g (267 mmol, 98%). ^1H NMR (600 MHz, CDCl_3): $\delta = 0.88$ (t, $J = 7.3$ Hz, 3 H, $-\text{CH}_3$), 1.22–1.32 [several peaks, 22 H, $-(\text{CH}_2)_{11}-$], 1.79 (d, $J = 3.2$ Hz, 1 H, OH), 3.79 (s, 6 H, OCH_3), 4.60 (m, 1 H, Ar-CH), 6.37 (t, $J = 2.3$ Hz, 1 H, Ar-4-H), and 6.51 ppm (d, $J = 2.3$ Hz, 2 H, Ar-2,6-H). HRMS (ESI-TOF): found $m/z = 359.2575$ ($[\text{M} + \text{Na}]^+$), calcd. for $\text{C}_{21}\text{H}_{36}\text{O}_3\text{Na}$, $m/z = 359.2557$.

1,3-Dimethoxy-5-tridecylbenzene (3): A solution of alcohol **2** (14.7 g, 44 mmol) in dry CH_2Cl_2 (1 L) was cooled to 0°C under nitrogen, to which trifluoroacetic acid (TFA) (49 mL, 656 mmol) and sodium cyanoborohydride (13.7 g, 219 mmol) were added, and the resulting mixture was stirred for 3 h. Then the reaction was quenched by the addition of ice water. The organic layer was separated and the aqueous layer was extracted with CH_2Cl_2 . The combined organic layer was washed with aqueous sodium carbonate and brine, dried with anhydrous sodium sulfate, and the solvents evaporated. The resulting yellow oil was separated by silica gel (Wakogel, C-200) column chromatography with hexane as an eluent to give **3** as a colorless solid. Yield 8.65 g (27 mmol, 62%). ^1H NMR (600 MHz, CDCl_3): $\delta = 0.88$ (t, $J = 6.8$ Hz, 3 H, $-\text{CH}_3$), 1.22–1.34 [several peaks, 22 H, $-(\text{CH}_2)_{11}-$], 2.54 (t, $J = 7.7$ Hz, 2 H, Ar- CH_2), 3.78 (s, 6 H, OCH_3), 6.29 (t, $J = 1.9$ Hz, 1 H, Ar-4-H), and 6.34 ppm (d, $J = 1.9$ Hz, 2 H, Ar-2,6-H). HRMS (FAB): found $m/z = 320.343$ (M^+), calcd. for $\text{C}_{21}\text{H}_{36}\text{O}_2$, $m/z = 320.272$.

2,6-Dimethoxy-4-tridecylbenzaldehyde (4): 3,5-Dimethoxy-1-tridecylbenzene (**3**, 56.1 g, 178 mmol) and *N,N,N',N'*-tetramethylethylenediamine (TMEDA) (160 mL) were dissolved in dry diethyl ether (500 mL). This solution was cooled to -78°C under nitrogen, and a white solid precipitated. Butyllithium (155 mL of 1.58 M solution in hexane, 246 mmol) was added dropwise to the solution, and the resulting mixture was stirred for 4 h. The color of the mixture gradually changed to orange, and then red. The reaction temperature was warmed to room temperature, and the mixture was stirred for an additional 3 h. The color of the mixture immediately changed to black. Then, dimethylformamide (DMF) (16.0 mL, 206 mmol) was added dropwise to the mixture and the resulting mixture was stirred for 2 h, which induced a color change to brown. The mixture was poured into ice water and the organic layer was separated. The aqueous layer was further extracted with diethyl ether, and the combined organic layer was washed with 3 M hydrochloric acid, saturated aqueous sodium hydrogen carbonate and brine, dried with anhydrous sodium sulfate, and the solvents evaporated. A solid precipitated during evaporation. The product **4** was obtained by recrystallization from ethyl acetate as the first crop. Further the filtrate was purified by silica gel (Wakogel C-300) column chromatography (AcOEt /hexane, 1:1) to give **4** as the second crop as a colorless solid. Yield 36.6 g (112 mmol, 56%). ^1H NMR (600 MHz, CDCl_3): $\delta = 0.88$ (t, $J = 6.8$ Hz, 3 H, $-\text{CH}_3$), 1.22–1.34 [several peaks, 20 H, $-(\text{CH}_2)_{10}-$], 1.63 (m, 2 H, Ar- CH_2CH_2), 2.60 (t, $J = 7.8$ Hz, 2 H, Ar- CH_2), 3.89 (s, 6 H, OCH_3), 6.38 (s, 2 H, Ar-H), and 10.45 (s, 1 H, CHO). HRMS (FAB): found $m/z = 349.331$ ($[\text{M} + \text{H}]^+$), calcd. for $\text{C}_{22}\text{H}_{36}\text{O}_3$, $m/z = 349.274$.

Methoxyphenyl-Substituted Porphyrin 6: The porphyrin **6** was prepared from the aldehyde **4** (7.18 g, 20.6 mmol) and dipyrromethane (**5**) (3.00 g, 20.6 mmol) according to the published method.^[22] Purple solid. Yield 2.91 g (3.07 mmol, 30%). ¹H NMR (600 MHz, CDCl₃): δ = −3.03 (s, 2 H, NH), 0.90 (t, J = 6.6 Hz, 6 H, −CH₃), 1.27–1.42 [several peaks, 28 H, −(CH₂)₇−], 1.45 (m, 4 H, −CH₂−), 1.52 (m, 4 H, −CH₂−), 1.59 (m, 4 H, −CH₂−), 1.96 (m, 4 H, −CH₂−), 2.95 (t, J = 7.8 Hz, 4 H, Ar-CH₂), 3.51 (s, 12 H, Ar-OCH₃), 6.87 (s, 4 H, Ar-H), 8.97 (d, J = 4.8 Hz, 4 H, β), 9.28 (d, J = 4.8 Hz, 4 H, β), and 10.14 ppm (s, 2 H, *meso*). HRMS (ESI-TOF): found m/z = 947.6405 ([M+H]⁺), calcd. for C₆₂H₈₃N₄O₄, m/z = 947.6409. UV/Vis (CHCl₃): λ_{\max} = 409, 503, 536, and 576 nm.

Hydroxyphenyl-Substituted Zn^{II}-Porphyrin 7: The porphyrin **6** (2.37 g, 2.50 mmol) was dissolved in dry CH₂Cl₂ (140 mL) and cooled to −78 °C under N₂, to which a solution of BBr₃ (25 g, 100 mmol) in dry CH₂Cl₂ (70 mL) was added slowly at −78 °C. The reaction mixture was stirred for 20 h at room temperature, poured into water, and neutralized with aqueous NaHCO₃. The organic layer was separated, washed with water and brine, and the solvents evaporated. The resulting purple solid was dissolved in methanol (1 L), and concd. hydrochloric acid (23 mL) was added. The resulting solution was stirred for 15 h under reflux, and then quenched with triethylamine (40 mL) and evaporated until the volume of the solution became ca. 500 mL. Then water was added to precipitate a purple solid. After filtration, the solid was dissolved in methanol (500 mL), stirred with Zn(OAc)₂ for 20 h at room temperature and evaporated until the volume of the solution became ca. 300 mL. Then, water was added to precipitate a purple solid, which was filtered and recrystallized (ethyl acetate/hexane) to give **7** (2.35 g, 98%). ¹H NMR (600 MHz, CDCl₃): δ = 0.90 (t, J = 6.8 Hz, 6 H, −CH₃), 1.26–1.41 [several peaks, 28 H, −(CH₂)₇−], 1.44 (m, 4 H, −CH₂−), 1.51 (m, 4 H, −CH₂−), 1.59 (m, 4 H, −CH₂−), 1.93 (m, 4 H, −CH₂−), 2.89 (t, J = 7.4 Hz, 4 H, Ar-CH₂), 4.67 (s, 4 H, Ar-OH), 6.87 (s, 4 H, Ar-H), 9.25 (d, J = 4.1 Hz, 4 H, β), 9.50 (d, J = 4.1 Hz, 4 H, β), and 10.36 ppm (s, 2 H, *meso*). HRMS (ESI-TOF): found m/z = 953.4813 ([M+H]⁺), calcd. for C₅₈H₇₃N₄O₄Zn, m/z = 953.4918. UV/Vis (CHCl₃): λ_{\max} = 413, 542, and 573 nm.

Doubly Strapped Zn^{II}-Porphyrin S1: The porphyrin **7** (621 mg, 651 μ mol), 1,10-dibromodecane (1.95 g, 6.51 mmol), and K₂CO₃ (5.40 g, 39.1 mmol) were dissolved in acetone (950 mL) under N₂, and the mixture was stirred for 20 days under reflux. The reaction mixture was filtered and the filtrate was evaporated. The resulting solid was dissolved in CHCl₃ (300 mL) and water (200 mL). The organic layer was separated, washed with brine, and dried with Na₂SO₄ and the solvents evaporated. Acetonitrile was added to the resulting solution and the mixture was filtered. The residue was purified by silica gel (Wakogel C-400) column chromatography (CH₂Cl₂/hexane, 7:3) and recrystallized from CHCl₃/acetonitrile to give the porphyrin **S1** (496 mg, 62%). ¹H NMR (600 MHz, CDCl₃): δ = −2.48 (m, 8 H, H^c), −1.44 (m, 8 H, H^d), −1.34 (m, 8 H, H^c), 0.65 (m, 8 H, H^b), 0.90 (t, J = 6.9 Hz, 6 H, −CH₃), 1.25–1.40 [several peaks, 28 H, −(CH₂)₇−], 1.43 (m, 4 H, −CH₂−), 1.50 (m, 4 H, −CH₂−), 1.59 (m, 4 H, −CH₂−), 1.93 (m, 4 H, −CH₂−), 2.93 (t, J = 7.3 Hz, 4 H, Ar-CH₂), 3.76 (t, J = 5.0 Hz, 8 H, H^a), 6.98 (s, 4 H, Ar-H), 9.11 (d, J = 4.1 Hz, 4 H, β), 9.37 (d, J = 4.1 Hz, 4 H, β), and 10.22 ppm (s, 2 H, *meso*). HRMS (ESI-TOF): found m/z = 1229.7733 ([M+H]⁺), calcd. for C₇₈H₁₀₈N₄O₄Zn, m/z = 1229.7735. UV/Vis (CHCl₃): λ_{\max} (ϵ) = 409 (404000) and 536 (21000) nm; fluorescence (CHCl₃): λ_{\max} = 575 and 631 nm.

5,15-Bis(2,6-dimethoxyphenyl)-Substituted Zn^{II}-Porphyrin M1: To a solution of **6** (100 mg, 105 μ mol) in CHCl₃ (10 mL) was added a

saturated solution of Zn(OAc)₂ in methanol, and the resulting mixture was stirred for 3 h. Then, water was added to the solution and the products were extracted with CHCl₃. The organic layer was washed with brine, dried with anhydrous sodium sulfate, and the solvents evaporated. The product was purified by silica-gel column chromatography with CH₂Cl₂/hexane and subsequent recrystallization from CHCl₃/acetonitrile, giving porphyrin **M1** (101 mg, 98%). ¹H NMR (600 MHz, CDCl₃): δ = 0.90 (t, J = 6.9 Hz, 6 H, −CH₃), 1.25–1.40 [several peaks, 32 H, −(CH₂)₈−], 1.46 (m, 4 H, −CH₂−), 1.63 (m, 4 H, −CH₂−), 1.97 (m, 4 H, −CH₂−), 2.97 (t, J = 7.3 Hz, 4 H, Ar-CH₂), 3.52 (s, 12 H, OMe), 6.88 (s, 4 H, Ar-H), 9.06 (d, J = 4.8 Hz, 4 H, β), 9.35 (d, J = 4.8 Hz, 4 H, β), and 10.19 ppm (s, 2 H, *meso*). HRMS (MALDI-TOF): found m/z = 1010.41, calcd. for C₆₂H₈₀N₄O₄Zn, m/z = 1010.69. UV/Vis (CHCl₃): λ_{\max} (ϵ) = 414 (404000) and 541 (17000) nm; fluorescence (CHCl₃): λ_{\max} = 584 and 635 nm.

General Procedure for Ag^I-Promoted *meso-meso* Coupling Reaction:

To a solution of *meso*-free Zn^{II}-porphyrin in dry CHCl₃ (1.0 mm) was added a stock solution of AgPF₆ in acetonitrile (0.12 M) under N₂ in the dark. The reaction mixture was stirred for appropriate time and the reaction was quenched by the addition of water. The organic layer was separated, washed with brine, dried with Na₂SO₄, and the solvents evaporated. The residue was passed through a short silica gel column and separated by GPC chromatography. Further purification by silica gel column chromatography (Wakogel C-400) and recrystallization from CHCl₃/acetonitrile provided *meso-meso*-linked oligomers.

Ag^I-Promoted *meso-meso* Coupling Reaction of S1: Following the general procedure (4 equiv. of AgPF₆, 48 h, under reflux), **S1** was coupled to provide **S2** (21%), **S3** (3%), and **S4** (trace) along with recovery of **S1** (52%). **S2:** ¹H NMR (600 MHz, CDCl₃): δ = −2.18 (m, 16 H, H^c), −1.25 (m, 16 H, H^d), −0.99 (m, 16 H, H^c), 0.77 (m, 16 H, H^b), 0.85 (t, J = 6.9 Hz, 12 H, −CH₃), 1.20–1.37 [several peaks, 56 H, −(CH₂)₇−], 1.40 (m, 8 H, −CH₂−), 1.48 (m, 8 H, −CH₂−), 1.58 (m, 8 H, −CH₂−), 1.82 (m, 8 H, −CH₂−), 2.82 (t, J = 7.7 Hz, 8 H, Ar-CH₂), 3.75 (m, 16 H, H^a), 6.89 (s, 8 H, Ar-H), 8.04 (d, J = 4.6 Hz, 4 H, β), 8.64 (d, J = 4.6 Hz, 4 H, β), 9.10 (d, J = 4.6 Hz, 4 H, β), 9.41 (d, J = 4.6 Hz, 4 H, β), and 10.25 ppm (s, 2 H, *meso*). HRMS (MALDI-TOF): found m/z = 2455.52, calcd. for C₁₅₆H₂₁₄N₈O₈Zn₂, m/z = 2452.75. UV/Vis (CHCl₃): λ_{\max} (ϵ) = 413 (231000), 446 (198000), 551 (59000), and 591 (18000) nm; fluorescence (CHCl₃): λ_{\max} = 593 and 650 nm. **S3:** ¹H NMR (600 MHz, CDCl₃): δ = −2.15 (m, 16 H, H^c), −1.84 (m, 8 H, H^c), −1.22 (m, 16 H, H^d), −1.01 (m, 16 H, H^c), −0.96 (m, 8 H, H^d), −0.71 (m, 8 H, H^c), 0.76–0.91 (m, 24 H, H^b), 0.79 (t, J = 6.8 Hz, 6 H, −CH₃), 0.87 (t, J = 10.1 Hz, 12 H, −CH₃), 1.12–1.39 [several peaks, 92 H, −(CH₂)_n−], 1.43 (m, 8 H, −CH₂−), 1.51 (m, 8 H, −CH₂−), 1.70 (m, 4 H, −CH₂−), 1.86 (m, 8 H, −CH₂−), 2.71 (t, J = 6.8 Hz, 4 H, Ar-CH₂), 2.86 (t, J = 6.9 Hz, 8 H, Ar-CH₂), 3.75 (t, J = 5.1 Hz, 8 H, H^a), 3.79 (t, J = 5.0 Hz, 16 H, H^a), 6.81 (s, 4 H, Ar-H), 6.93 (s, 8 H, Ar-H), 8.08 (d, J = 4.6 Hz, 4 H, β), 8.19 (d, J = 4.6 Hz, 4 H, β), 8.63 (d, J = 4.6 Hz, 4 H, β), 8.73 (d, J = 4.6 Hz, 4 H, β), 9.14 (d, J = 4.1 Hz, 4 H, β), 9.43 (d, J = 4.1 Hz, 4 H, β), and 10.28 ppm (s, 2 H, *meso*). HRMS (MALDI-TOF): found m/z = 3685.28, calcd. for C₂₃₄H₃₂₀N₁₂O₁₂Zn₃, m/z = 3682.27. UV/Vis (CHCl₃): λ_{\max} (ϵ) = 410 (358000), 471 (278000), 561 (110000), and 601 (40000) nm; fluorescence (CHCl₃): λ_{\max} = 603 and 659 nm. **S4:** ¹H NMR (600 MHz, CDCl₃): δ = −2.13 (m, 16 H, H^c), −1.81 (m, 16 H, H^c), −1.20 (m, 16 H, H^d), −1.00 (m, 16 H, H^c), −0.96 (m, 16 H, H^d), −0.66 (m, 16 H, H^c), 0.81 (t, J = 6.8 Hz, 12 H, −CH₃), 0.82 (m, 16 H, H^b), 0.87 (t, J = 6.9 Hz, 12 H, −CH₃), 0.92 (m, 16 H, H^b), 1.13–1.34 [several peaks, 136 H, −(CH₂)_n−], 1.37 (m, 8 H, −CH₂−), 1.43 (m, 8 H, −CH₂−), 1.52 (m, 8 H, −CH₂−), 1.74 (m, 8 H, −CH₂−),

1.87 (m, 8 H, $-\text{CH}_2-$), 2.74 (t, $J = 7.8$ Hz, 8 H, Ar- CH_2), 2.86 (t, $J = 7.4$ Hz, 8 H, Ar- CH_2), 3.80 (t, $J = 5.1$ Hz, 16 H, H^a), 3.81 (t, $J = 5.0$ Hz, 16 H, H^a), 6.85 (s, 8 H, Ar-H), 6.94 (s, 8 H, Ar-H), 8.10 (d, $J = 4.6$ Hz, 4 H, β), 8.21 (d, $J = 4.6$ Hz, 4 H, β), 8.22 (d, $J = 4.6$ Hz, 4 H, β), 8.67 (d, $J = 4.6$ Hz, 4 H, β), 8.72 (d, $J = 4.6$ Hz, 4 H, β), 8.74 (d, $J = 4.6$ Hz, 4 H, β), 9.15 (d, $J = 4.1$ Hz, 4 H, β), 9.44 (d, $J = 4.1$ Hz, 4 H, β), and 10.29 ppm (s, 2 H, *meso*). HRMS (MALDI-TOF): found $m/z = 4908.75$, calcd. for $\text{C}_{312}\text{H}_{426}\text{N}_{16}\text{O}_{16}\text{Zn}_4$, $m/z = 4909.02$. UV/Vis (CHCl_3): λ_{max} (ϵ) = 411 (408000), 484 (348000), 568 (148000), and 606 (32000) nm; fluorescence (CHCl_3): λ_{max} = 608 and 662 nm.

Ag^I-Promoted *meso-meso* Coupling Reaction of S2: Following the general procedure (4 equiv. of AgPF_6 , 48 h, under reflux), **S2** was coupled to provide **S4** (21%), **S6** (4%), and **S8** (trace) along with recovery of **S2** (57%). **S6**: ^1H NMR (600 MHz, CDCl_3): $\delta = -2.12$ (m, 16 H, H^c), -1.77 (m, 16 H, H^c), -1.75 (m, 16 H, H^c), -1.19 (m, 16 H, H^d), -0.97 (m, 32 H, H^d), -0.97 (m, 16 H, H^c), -0.62 (m, 32 H, H^c), 0.81 (t, $J = 7.8$ Hz, 12 H, $-\text{CH}_3$), 0.82 (m, 16 H, H^b), 0.83 (t, $J = 6.8$ Hz, 12 H, $-\text{CH}_3$), 0.88 (t, $J = 6.4$ Hz, 12 H, $-\text{CH}_3$), 0.95 (m, 32 H, H^b), 1.14–1.47 [several peaks, 232 H, $-(\text{CH}_2)_n-$], 1.53 (m, 8 H, $-\text{CH}_2-$), 1.77 (m, 16 H, $-\text{CH}_2-$), 1.88 (m, 8 H, $-\text{CH}_2-$), 2.75 (t, $J = 7.3$ Hz, 8 H, Ar- CH_2), 2.78 (t, $J = 6.8$ Hz, 8 H, Ar- CH_2), 2.87 (t, $J = 7.4$ Hz, 8 H, Ar- CH_2), 3.80–3.84 (three peaks of t, 48 H, H^a), 6.86 (s, 8 H, Ar-H), 6.90 (s, 8 H, Ar-H), 6.95 (s, 8 H, Ar-H), 8.11 (d, $J = 4.6$ Hz, 4 H, β), 8.23 (d, $J = 4.6$ Hz, 4 H, β), 8.24–8.28 (three peaks of d, 12 H, β), 8.67 (d, $J = 4.6$ Hz, 4 H, β), 8.73–8.78 (four peaks of d, 16 H, β), 9.15 (d, $J = 4.1$ Hz, 4 H, β), 9.44 (d, $J = 4.1$ Hz, 4 H, β), and 10.29 ppm (s, 2 H, *meso*). HRMS (MALDI-TOF): found $m/z = 7363.33$, calcd. for $\text{C}_{468}\text{H}_{638}\text{N}_{24}\text{O}_{24}\text{Zn}_6$, $m/z = 7362.52$. UV/Vis (CHCl_3): λ_{max} (ϵ) = 411 (557000), 494 (514000), 572 (268000), and 611 (93000) nm; fluorescence (CHCl_3): λ_{max} = 611 and 662 nm. **S8**: ^1H NMR (600 MHz, CDCl_3): $\delta = -2.11$ (m, 16 H, H^c), -1.77 (m, 16 H, H^c), -1.74 (m, 32 H, H^c), -1.19 (m, 16 H, H^d), -0.94 (m, 64 H, H^d and H^c), -0.60 (m, 48 H, H^c), 0.80–0.89 (several peaks, 64 H, H^b and $-\text{CH}_3$), 0.94 (m, 16 H, H^b), 0.99 (m, 32 H, H^b), 1.14–1.38 [several peaks, 288 H, $-(\text{CH}_2)_n-$], 1.43 (m, 24 H, $-\text{CH}_2-$), 1.60 (m, 8 H, $-\text{CH}_2-$), 1.77 (m, 24 H, $-\text{CH}_2-$), 1.88 (m, 8 H, $-\text{CH}_2-$), 2.74–2.80 (three peaks of t, 24 H, Ar- CH_2), 2.87 (t, $J = 6.4$ Hz, 8 H, Ar- CH_2), 3.78–3.87 (four peaks of t, 64 H, H^a), 6.86 (s, 8 H, Ar-H), 6.90 (s, 8 H, Ar-H), 6.91 (s, 8 H, Ar-H), 6.95 (s, 8 H, Ar-H), 8.12 (d, $J = 4.6$ Hz, 4 H, β), 8.23 (d, $J = 4.6$ Hz, 4 H, β), 8.24–8.29 (five peaks of d, 20 H, β), 8.68 (d, $J = 4.6$ Hz, 4 H, β), 8.74–8.79 (six peaks of d, 24 H, β), 9.15 (d, $J = 4.1$ Hz, 4 H, β), 9.45 (d, $J = 4.1$ Hz, 4 H, β), and 10.29 ppm (s, 2 H, *meso*). HRMS (MALDI-TOF): found $m/z = 9824.21$, calcd. for $\text{C}_{624}\text{H}_{850}\text{N}_{32}\text{O}_{32}\text{Zn}_8$, $m/z = 9826.10$. UV/Vis (CHCl_3): λ_{max} (ϵ) = 411 (529000), 498 (520000), 574 (304000), and 612 (114000) nm; fluorescence (CHCl_3): λ_{max} = 612 and 663 nm.

Ag^I-Promoted *meso-meso* Coupling Reaction of S4: Following the general procedure (9 equiv. of AgPF_6 , 48 h, at 40 °C), **S4** was coupled to provide **S8** (10%), **S12** (5%), and **S16** (trace) along with recovery of **S4** (33%). **S12**: ^1H NMR (600 MHz, CDCl_3): $\delta = -2.11$ (m, 16 H, H^c), -1.77 (m, 16 H, H^c), -1.72 (m, 64 H, H^c), -1.19 (m, 16 H, H^d), -0.94 (m, 96 H, H^d and H^c), -0.57 (m, 80 H, H^c), 0.80–0.89 (several peaks, 88 H, H^b and $-\text{CH}_3$), 0.94 (m, 16 H, H^b), 0.99 (m, 64 H, H^b), 1.14–1.38 [several peaks, 432 H, $-(\text{CH}_2)_n-$], 1.43 (m, 40 H, $-\text{CH}_2-$), 1.60 (m, 8 H, $-\text{CH}_2-$), 1.77 (m, 40 H, $-\text{CH}_2-$), 1.88 (m, 8 H, $-\text{CH}_2-$), 2.74–2.80 (several peaks, 40 H, Ar- CH_2), 2.87 (m, 8 H, Ar- CH_2), 3.78–3.87 (six peaks of t, 96 H, H^a), 6.86 (s, 8 H, Ar-H), 6.90 (s, 8 H, Ar-H), 6.92 (s, 24 H, Ar-H), 6.95 (s, 8 H, Ar-H), 8.12 (d, $J = 4.6$ Hz, 4 H, β), 8.23 (d, $J = 4.6$ Hz, 4 H, β), 8.24–8.29 (nine peaks of d, 36 H, β), 8.68 (d, $J = 4.6$ Hz, 4 H, β),

8.74–8.79 (ten peaks of d, 40 H, β), 9.15 (d, $J = 4.1$ Hz, 4 H, β), 9.45 (d, $J = 4.1$ Hz, 4 H, β), and 10.29 ppm (s, 2 H, *meso*). HRMS (MALDI-TOF): found $m/z = 14742.72$, calcd. for $\text{C}_{936}\text{H}_{1274}\text{N}_{48}\text{O}_{48}\text{Zn}_{12}$, $m/z = 14750.71$. UV/Vis (CHCl_3): λ_{max} (ϵ) = 411 (587000), 502 (586000), 576 (379000), and 614 (174000) nm; fluorescence (CHCl_3): λ_{max} = 613 and 663 nm.

General Procedure for Bromination of Sn: To a solution of **Sn** (10 mg) in CHCl_3 (10 mL) was added 2.2 equiv. of NBS. After the reaction mixture was stirred at 0 °C for 1 h, the reaction was quenched by addition of water. The organic layer was separated, washed with brine, dried with Na_2SO_4 , and the solvent was evaporated. The resulting residue was passed through a short silica gel column. Recrystallization from a mixture of CHCl_3 and acetonitrile gave **BSn**.

General Procedure for Phenyl Capping Reaction of BSn: To a solution of **BSn** (10 mg) in dry toluene (10 mL) was added $\text{PhB}(\text{OH})_2$ (10 equiv.), $\text{Pd}(\text{PPh}_3)_4$ (0.1 equiv.), and K_2CO_3 (20 equiv.) and the resulting mixture was degassed by three times of freeze-pump-degassing cycles and stirred for 8 h under reflux under N_2 . After the reaction was quenched by the addition of water, the organic layer was separated, washed with brine, dried with Na_2SO_4 , and the solvent was evaporated. After the resulting residue was passed through a short silica gel column, recrystallization from a mixture of CHCl_3 and acetonitrile provided **PSn**.

General Procedure for DDQ-Sc(OTf)₃ Oxidation: To a solution of **PSn** (10 mg) in dry toluene (10 mL) was added 4 equiv. of DDQ and 4 equiv. of $\text{Sc}(\text{OTf})_3$. The resulting reaction mixture was stirred at 80 °C for 2 h under N_2 in the dark and the reaction was quenched by the addition of THF. The resulting mixture was passed through a short alumina column and the solvent was evaporated. Recrystallization from a mixture of CHCl_3 and acetonitrile provided **TSn**.

Following the general procedure, **TS2** was prepared from **PS2** in 92% yield as red-purple solid. ^1H NMR (600 MHz, CDCl_3): $\delta = -0.38$ (m, 16 H, H^c), 0.07 (m, 16 H, H^d), 0.11 (m, 16 H, H^c), 0.89 (t, $J = 6.9$ Hz, 12 H, $-\text{CH}_3$), 1.15 (m, 16 H, H^b), 1.24–1.38 [several peaks, 64 H, $-(\text{CH}_2)_8-$], 1.43 (m, 8 H, $-\text{CH}_2-$), 1.49 (m, 8 H, $-\text{CH}_2-$), 1.81 (m, 8 H, $-\text{CH}_2-$), 2.78 (t, $J = 7.3$ Hz, 8 H, Ar- CH_2), 3.82 (m, 8 H, H^a), 3.88 (m, 8 H, H^a), 6.74 (s, 8 H, Ar-H), 7.23 (s, 4 H, β), 7.54 (m, 2 H, Ph-*p*-H), 7.55 (m, 4 H, Ph-*m*-H), 7.60 (d, $J = 4.6$ Hz, 4 H, β), 7.62 (d, $J = 4.6$ Hz, 4 H, β), and 7.79 ppm (m, 4 H, Ph-*o*-H). HRMS (MALDI-TOF): found $m/z = 2598.64$, calcd. for $\text{C}_{168}\text{H}_{218}\text{N}_4\text{O}_4\text{Zn}_2$, $m/z = 2608.29$. UV/Vis (CHCl_3): λ_{max} (ϵ) = 416 (112000), 554 (74000), 586 (87000), 895 (13000), and 1024 (23000) nm.

Following the general procedure, **TS3** was prepared from **PS3** in 87% yield as a green solid. ^1H NMR (600 MHz, CDCl_3 , 60 °C): $\delta = -0.74$ (m, 24 H, H^c), -0.14 (m, 48 H, H^c and H^d), 0.76 (m, 24 H, H^b), 0.93 (m, 18 H, $-\text{CH}_3$), 1.24–1.55 [several peaks, 120 H, $-(\text{CH}_2)_{10}-$], 1.82 (m, 8 H, $-\text{CH}_2-$), 2.78 (m, 8 H, Ar- CH_2), 3.67 (m, 8 H, H^a), 3.75 (m, 8 H, H^a), 3.89 (m, 8 H, H^a), 6.34 (br., 4 H, β), 6.62 (s, 4 H, Ar-H), 6.66 (s, 8 H, Ar-H), 7.04 (br., 4 H, β), 7.47 (several peaks, 14 H, β , Ph-*m*-H and Ph-*p*-H), and 7.79 ppm (m, 4 H, Ph-*o*-H). HRMS (MALDI-TOF): found $m/z = 3825.16$, calcd. for $\text{C}_{246}\text{H}_{320}\text{N}_{12}\text{O}_{12}\text{Zn}_3$, $m/z = 3833.30$. UV/Vis (CHCl_3): λ_{max} = 418, 676, 1114, and 1294 nm.

Following the general procedure, **TS4** was prepared from **PS4** in 74% yield as a green solid. HRMS (MALDI-TOF): found $m/z = 5048.66$, calcd. for $\text{C}_{324}\text{H}_{422}\text{N}_{16}\text{O}_{16}\text{Zn}_4$, $m/z = 5058.32$. UV/Vis (CHCl_3): λ_{max} = 504, 716, 1282, and 1466 nm.

Following the general procedure, **TS6** was prepared from **PS6** in 95% yield as green solid. UV/Vis (CHCl₃): λ_{max} = 400, 770, 1556, and 1772 nm.

Following the general procedure, **TS8** was prepared from **PS8** in 78% yield as a green solid. UV/Vis (CHCl₃): λ_{max} = 406, 830, and 1982 nm.

Following the general procedure, **TS12** was prepared from **PS12** in 62% yield as a green solid.

Crystallographic Data Collection and Structure Refinement: Data collection for the **S1** was carried out at –150 °C with a Rigaku Raxis-Rapid with graphite-monochromated Mo- K_{α} radiation (λ = 0.71069 Å). Data collection for the compounds **S2** was carried out at –183 °C on a Bruker SMART APEX with graphite-monochromated Mo- K_{α} radiation (λ = 0.71069 Å). Details of the X-ray measurements are given in Table 1. The structures were solved by direct methods (Sir 97^[23] or SHELXS-97^[24]) and refined with Rigaku CrystalStructure software or with full-matrix least square procedures on F^2 for all reflections (SHELXL-97).^[24]

Table 1. Crystal data and structure refinements of **S1** and **S2**.

	S1	S2
Formula	C ₇₈ H ₁₀₈ N ₄ O ₄ Zn	C ₁₅₆ H ₂₁₄ N ₈ O ₈ Zn ₂
M_r	1231.05	2460.22
T [K]	123	90(2)
Crystal system	monoclinic	monoclinic
Space group	$P2_1/c$	$P2_1/n$
a [Å]	14.1291(5)	13.0780(17)
b [Å]	10.2235(3)	33.438(5)
c [Å]	23.1373(7)	31.055(4)
α [°]	90	90
β [°]	90.1800(11)	92.556(8)
γ [°]	90	90
V [Å ³]	3342.14(18)	13567(3)
Z	2	4
$\rho_{\text{calcd.}}$ [g cm ^{–3}]	1.223	1.204
μ [cm ^{–1}]	4.21	4.15
$F(000)$	1332	5320
Crystal size [mm]	0.70 × 0.40 × 0.10	0.70 × 0.30 × 0.10
$2\theta_{\text{max}}$ [°]	55.0	55.0
Observed reflections	7533	19542
Total reflections	24488	52792
Parameters	395	1580
R_1 [$I > 2\sigma(I)$]	0.0755	0.0750
wR_2 [$I > 2\sigma(I)$]	0.1945	0.1866
GOF	1.359	0.979

CCDC-299457 (for **S1**), and -299458 (for **S2**) contain the supplementary crystallographic data for this paper. These data can be obtained free of charge from The Cambridge Crystallographic Data Centre via www.ccdc.cam.ac.uk/data_request/cif.

Supporting Information (see footnote on the first page of this article): Experimental procedure and spectroscopic data for **Mn**, **BSn**, and **PSn**, and UV/Vis absorption spectra of **Sn** and **Mn**.

- [1] a) R. E. Martin, F. Diederich, *Angew. Chem.* **1999**, *111*, 1440; *Angew. Chem. Int. Ed.* **1999**, *38*, 1350; b) J. M. Tour, *Chem. Rev.* **1996**, *96*, 537; c) P. F. H. Schwab, M. D. Levin, J. Michl, *Chem. Rev.* **1999**, *99*, 1863; d) J. Cornil, D. Beljonne, J.-P. Calbert, J.-L. Brédas, *Adv. Mater.* **2001**, *13*, 1053; e) A. Kraft, A. C. Grimsdale, A. B. Holmes, *Angew. Chem.* **1998**, *110*, 416; *Angew. Chem. Int. Ed.* **1998**, *37*, 402; f) J. S. Moore, *Acc. Chem. Res.* **1997**, *30*, 402; g) D. T. McQuade, A. E. Pullen, T. M. Swager, *Chem. Rev.* **2000**, *100*, 2537; h) U. H. F. Bunz, *Chem. Rev.* **2000**, *100*, 1605; i) M. D. Watson, A. Fechtenkötter, K. Müllen, *Chem. Rev.* **2001**, *101*, 1267; j) F. Diederich, *Chem. Commun.* **2001**, 219.
- [2] a) P. Liess, V. Hensel, A. D. Schlüter, *Liebigs Ann.* **1996**, 1037; b) U. Stalmach, H. Kolshorn, I. Brehm, H. Meier, *Liebigs Ann.* **1996**, 1449; c) R. E. Martin, U. Gubler, J. Cornil, M. Balakina, C. Boudon, C. Bosshard, J.-P. Gisselbrecht, F. Diederich, P. Günter, M. Gross, J.-L. Brédas, *Chem. Eur. J.* **2000**, *6*, 3622; d) N. Sumi, H. Nakanishi, S. Ueno, K. Takimiya, Y. Aso, T. Otsubo, *Bull. Chem. Soc. Jpn.* **2001**, *74*, 979; e) T. Izumi, S. Kobashi, K. Takimiya, Y. Aso, T. Otsubo, *J. Am. Chem. Soc.* **2003**, *125*, 5286; f) T. Gbitter, F. Hampel, J.-P. Gisselbrecht, A. Hirsch, *Chem. Eur. J.* **2002**, *8*, 408; g) L. Dunsch, P. Rapt, N. Schulte, A. D. Schlüter, *Angew. Chem.* **2002**, *114*, 2187; *Angew. Chem. Int. Ed.* **2002**, *41*, 2082; h) S. Toyata, M. Goichi, M. Kotani, *Angew. Chem.* **2004**, *116*, 2298; *Angew. Chem. Int. Ed.* **2004**, *43*, 2248; i) W.-S. Li, D.-L. Jiang, T. Aida, *Angew. Chem.* **2004**, *116*, 3003; *Angew. Chem. Int. Ed.* **2004**, *43*, 2943; j) Q. Zheng, J. A. Gladysz, *J. Am. Chem. Soc.* **2005**, *127*, 10508.
- [3] a) H. Meier, *Angew. Chem.* **2005**, *117*, 2536; *Angew. Chem. Int. Ed.* **2005**, *44*, 2482; b) E. Clar, *Ber. Dtsch. Chem. Ges.* **1936**, *69*, 607; c) H. Meier, U. Stalmach, H. Kolshorn, *Acta Polym.* **1997**, *48*, 379; d) S. Eisler, A. D. Slepov, E. Elliott, T. Luu, R. McDonald, F. A. Hegmann, R. R. Tykwinski, *J. Am. Chem. Soc.* **2005**, *127*, 2666.
- [4] J.-H. Chou, M. E. Kosal, H. S. Nalwa, N. A. Rakow, K. S. Suslick, *The Porphyrin Handbook* (Eds.: K. M. Kadish, K. M. Smith, R. Guilard), Academic Press, San Diego, **2000**, Vol. 6, Chapter 41.
- [5] a) D. P. Arnold, A. W. Johnson, M. Mahendran, *J. Chem. Soc., Perkin Trans. 1* **1978**, 366; b) D. P. Arnold, G. A. Heath, *J. Am. Chem. Soc.* **1993**, *115*, 12197.
- [6] a) V. S. Y. Lin, S. G. DiMugno, M. J. Therien, *Science* **1994**, *264*, 1105; b) S. M. LeCour, H.-W. Guan, S. G. DiMugno, C. H. Wang, M. J. Therien, *J. Am. Chem. Soc.* **1996**, *118*, 1497; c) H. T. Uyeda, Y. Zhao, K. Wostyn, I. Asselberghs, K. Clays, A. Persoons, M. J. Therien, *J. Am. Chem. Soc.* **2002**, *124*, 13806; d) K. Susumu, T. V. Duncan, M. J. Therien, *J. Am. Chem. Soc.* **2005**, *127*, 5186.
- [7] a) H. L. Anderson, *Chem. Commun.* **1999**, 2323; b) P. N. Taylor, A. P. Wylie, J. Huuskonen, H. L. Anderson, *Angew. Chem.* **1998**, *110*, 1033; *Angew. Chem. Int. Ed.* **1998**, *37*, 986; c) I. M. Blake, H. L. Anderson, D. Beljonne, J.-L. Brédas, W. Clegg, *J. Am. Chem. Soc.* **1998**, *120*, 10764; d) I. M. Blake, L. H. Rees, T. D. W. Claridge, H. L. Anderson, *Angew. Chem.* **2000**, *112*, 1888; *Angew. Chem. Int. Ed.* **2000**, *39*, 1818.
- [8] a) M. G. H. Vicente, L. Jaquinod, K. M. Smith, *Chem. Commun.* **1999**, 1771; b) L. Jaquinod, O. Siri, R. G. Khoury, K. M. Smith, *Chem. Commun.* **1998**, 1261; c) M. G. H. Vicente, M. T. Cancilla, C. B. Lebrilla, K. M. Smith, *Chem. Commun.* **1998**, 2355; d) R. Paolesse, L. Jaquinod, F. D. Sala, D. J. Nurco, L. Prodi, M. Montalti, C. D. Natale, A. D'Amico, A. D. Carlo, P. Lugli, K. M. Smith, *J. Am. Chem. Soc.* **2000**, *122*, 11295; e) H. Aihara, L. Jaquinod, D. J. Nurco, K. M. Smith, *Angew. Chem.* **2001**, *113*, 3547; *Angew. Chem. Int. Ed.* **2001**, *40*, 3439; f) M. Nath, J. C. Huffman, J. M. Zaleski, *J. Am. Chem. Soc.* **2003**, *125*, 11484.
- [9] a) M. J. Crossley, P. L. Burn, *J. Chem. Soc., Chem. Commun.* **1991**, 1569; b) K. Sendt, L. A. Johnston, W. A. Hough, M. J. Crossley, N. S. Hush, J. R. Reimers, *J. Am. Chem. Soc.* **2002**, *124*, 9299.
- [10] a) N. Ono, H. Hironaga, K. Ono, S. Kaneko, T. Murashima, T. Ueda, C. Tsukamura, T. Ogawa, *J. Chem. Soc., Perkin Trans. 1* **1996**, 417; b) S. Ito, T. Murashima, N. Ono, H. Uno, *Chem. Commun.* **1998**, 1661; c) H. Uno, A. Masumoto, N. Ono, *J. Am. Chem. Soc.* **2003**, *125*, 12082; d) O. S. Finikova, A. V. Cheprakov, I. P. Beletskaya, P. J. Carroll, S. A. Vinogradov, *J. Org. Chem.* **2004**, *69*, 522; e) K. Sugiura, T. Matsumoto, S. Ohkouchi, Y. Naitoh, T. Kawai, Y. Takai, K. Ushiroda, Y. Sakata, *Chem. Commun.* **1999**, 1957; f) O. Yamane, K. Sugiura, H. Miyasaka, K. Nakamura, T. Fujimoto, K. Nakamura, T.

- Kaneda, Y. Sakata, M. Yamashita, *Chem. Lett.* **2004**, 33, 40; g) A. N. Cammidge, P. J. Scaife, G. Berber, D. L. Hughes, *Org. Lett.* **2005**, 7, 3413; h) T. D. Lash, P. Chandrasekar, *J. Am. Chem. Soc.* **1996**, 118, 8767; i) T. D. Lash, S. T. Chaney, *Angew. Chem.* **1997**, 109, 867; *Angew. Chem. Int. Ed. Engl.* **1997**, 36, 839.
- [11] a) A. Tsuda, A. Nakano, H. Furuta, H. Yamochi, A. Osuka, *Angew. Chem.* **2000**, 112, 572; *Angew. Chem. Int. Ed.* **2000**, 39, 558; b) A. Tsuda, H. Furuta, A. Osuka, *Angew. Chem.* **2000**, 112, 2649; *Angew. Chem. Int. Ed.* **2000**, 39, 2549; c) A. Tsuda, H. Furuta, A. Osuka, *J. Am. Chem. Soc.* **2001**, 123, 10304; d) A. Tsuda, A. Osuka, *Science* **2001**, 293, 79; e) S. Hiroto, A. Osuka, *J. Org. Chem.* **2005**, 70, 4054; f) T. Ikeue, N. Aratani, A. Osuka, *Isr. J. Chem.* **2005**, 45, 293.
- [12] a) D. Bonifazi, M. Scholl, F. Song, L. Echegoyen, G. Accorsi, N. Armaroli, F. Diederich, *Angew. Chem.* **2003**, 115, 5116; *Angew. Chem. Int. Ed.* **2003**, 42, 4966; b) N. Armaroli, G. Accorsi, F. Song, A. Palkar, L. Echegoyen, D. Bonifazi, F. Diederich, *ChemPhysChem* **2005**, 6, 732; c) D. Bonifazi, G. Accorsi, N. Armaroli, F. Song, A. Palkar, L. Echegoyen, M. Scholl, P. Seiler, B. Jaun, F. Diederich, *Helv. Chim. Acta* **2005**, 88, 1839.
- [13] a) D. Bonifazi, H. Spillmann, A. Kiebele, M. de Wild, P. Seiler, F. Cheng, H.-J. Güntherlodt, T. Jung, F. Diederich, *Angew. Chem.* **2004**, 116, 4863; *Angew. Chem. Int. Ed.* **2004**, 43, 4759; b) H. Sato, K. Tashiro, H. Shinmori, A. Osuka, T. Aida, *Chem. Commun.* **2005**, 2324; c) H. Sato, K. Tashiro, H. Shinmori, A. Osuka, Y. Murata, K. Komatsu, T. Aida, *J. Am. Chem. Soc.* **2005**, 127, 13086.
- [14] a) J.-S. Yang, T. Swager, *J. Am. Chem. Soc.* **1998**, 120, 11864; b) T. Sato, D.-L. Jiang, T. Aida, *J. Am. Chem. Soc.* **1999**, 121, 10658; c) D.-L. Jiang, C.-K. Choi, K. Honda, W.-S. Li, T. Yuzawa, T. Aida, *J. Am. Chem. Soc.* **2004**, 126, 12084; d) J. J. Michels, M. J. O'Connell, P. N. Taylor, J. S. Wilson, F. Cacialli, H. L. Anderson, *Chem. Eur. J.* **2003**, 9, 6167; e) P. N. Taylor, A. J. Hagan, H. L. Anderson, *Org. Biomol. Chem.* **2003**, 1, 3851.
- [15] a) T. Nagata, *Bull. Chem. Soc. Jpn.* **1992**, 65, 385; b) A. Osuka, T. Okada, S. Taniguchi, K. Nozaki, T. Ohno, N. Mataga, *Tetrahedron Lett.* **1995**, 36, 5781.
- [16] a) A. Osuka, H. Shimidzu, *Angew. Chem.* **1997**, 109, 93; *Angew. Chem. Int. Ed. Engl.* **1997**, 36, 135; b) A. Nakano, A. Osuka, I. Yamazaki, T. Yamazaki, Y. Nishimura, *Angew. Chem.* **1998**, 110, 3172; *Angew. Chem. Int. Ed.* **1998**, 37, 3023; c) N. Aratani, A. Osuka, Y. H. Kim, D. H. Jeong, D. Kim, *Angew. Chem.* **2000**, 112, 1517; *Angew. Chem. Int. Ed.* **2000**, 39, 1458; d) A. Nakano, T. Yamazaki, Y. Nishimura, I. Yamazaki, A. Osuka, *Chem. Eur. J.* **2000**, 6, 3254; e) N. Aratani, A. Takagi, Y. Yanagawa, T. Matsumoto, T. Kawai, Z. S. Yoon, D. Kim, A. Osuka, *Chem. Eur. J.* **2005**, 11, 3389.
- [17] a) Y. H. Kim, D. H. Jeong, D. Kim, S. C. Jeoung, H. S. Cho, S. K. Kim, N. Aratani, A. Osuka, *J. Am. Chem. Soc.* **2001**, 123, 76; b) D. H. Jeong, S. M. Jang, I.-W. Hwang, D. Kim, N. Yoshida, A. Osuka, *J. Phys. Chem. A* **2002**, 106, 11054; c) N. Yoshida, T. Ishizuka, A. Osuka, D. H. Jeong, H. S. Cho, D. Kim, Y. Matsuzaki, A. Nogami, K. Tanaka, *Chem. Eur. J.* **2003**, 9, 58.
- [18] a) H. S. Cho, D. H. Jeong, S. Cho, D. Kim, Y. Matsuzaki, K. Tanaka, A. Tsuda, A. Osuka, *J. Am. Chem. Soc.* **2002**, 124, 14642; b) T. Miyahara, H. Nakatsuji, J. Hasegawa, A. Osuka, N. Aratani, A. Tsuda, *J. Chem. Phys.* **2002**, 117, 11196.
- [19] P. G. Seybold, M. Gouterman, *J. Mol. Spectrosc.* **1969**, 31, 1.
- [20] M.-C. Yoon, D. H. Jeong, S. Cho, D. Kim, H. Rhee, T. Joo, *J. Chem. Phys.* **2003**, 118, 164.
- [21] a) Y.-C. Lu, E. W.-G. Diau, H. Rau, *J. Phys. Chem. A* **2005**, 109, 2090; b) M. Maus, W. Rettig, D. Bonafoux, R. Lapouyade, *J. Phys. Chem. A* **1999**, 103, 3388; c) M. Maus, W. Rettig, *J. Phys. Chem. A* **2002**, 106, 2104; d) J. Chen, B. Xu, X. Ouyang, B. Z. Tang, Y. Cao, *J. Chem. Phys. A* **2004**, 108, 7522.
- [22] B. J. Littler, Y. Ciringh, J. S. Lindsey, *J. Org. Chem.* **1999**, 64, 2864.
- [23] A. Altomare, M. C. Burla, M. Camalli, G. L. Cascarano, C. Giacovazzo, A. Guagliardi, A. G. G. Moliterni, G. Polidori, R. Spagna, *J. Appl. Crystallogr.* **1999**, 32, 115.
- [24] G. M. Sheldrick, SHELX-97, program for the Refinement of Crystal Structures, University of Göttingen, Göttingen, Germany, **1997**.

Received: April 1, 2006

Published Online: May 9, 2006